Neuroscience Research 75 (2013) 59–64

Contents lists available at SciVerse ScienceDirect

Neuroscience Research

journal homepage: www.elsevier.com/locate/neures

Technical note

Parallel and patterned optogenetic manipulation of neurons in the brain slice using a DMD-based projector

Seiichiro Sakai[a,b,c,d], Kenichi Ueno[e], Toru Ishizuka[a,b], Hiromu Yawo[a,b,c,f,*]

[a] Department of Developmental Biology and Neuroscience, Tohoku University Graduate School of Life Sciences, Sendai 980-8577, Japan
[b] JST, CREST, Tokyo 102-0075, Japan
[c] Tohoku University Basic and Translational Research Centre for Global Brain Science, Sendai 980-8575, Japan
[d] Japan Society for the Promotion of Science, Tokyo 102-8472, Japan
[e] CS Center, ASKA Company, Katou 679-0221, Japan
[f] Center for Neuroscience, Tohoku University Graduate School of Medicine, Sendai 980-8575, Japan

ARTICLE INFO

Article history:
Received 29 December 2011
Received in revised form 22 February 2012
Accepted 28 February 2012
Available online 24 March 2012

Keywords:
Optics
Light stimulation
Brain slice
Channelrhodopsin
Archaerhodopsin
Optogenetics
Microscope
Software

ABSTRACT

Optical manipulation technologies greatly advanced the understanding of the neuronal network and its dysfunctions. To achieve patterned and parallel optical switching, we developed a microscopic illumination system using a commercial DMD-based projector and a software program. The spatiotemporal patterning of the system was evaluated using acute slices of the hippocampus. The neural activity was optically manipulated, positively by the combination of channelrhodopsin-2 (ChR2) and blue light, and negatively by the combination of archaerhodopsin-T (ArchT) and green light. It is suggested that our projector-managing optical system (PMOS) would effectively facilitate the optogenetic analyses of neurons and their circuits.

© 2012 Elsevier Ireland Ltd and the Japan Neuroscience Society. All rights reserved.

The brain consists of many types of neurons which make a complex network. Although this idea was first proposed by Ramon y Cajal more than 100 years ago, it is still unresolved how the network activities are integrated in the brain. The brain's network performance has been investigated through the analysis of its input–output relationship. Conventionally, the input signals are given electrically using electrodes placed in the extracellular space. Although with this method it is easy to control the temporal pattern of activation, many neurons and axons in the relatively broad field are stimulated simultaneously. Moreover, the electrical field is generally nonuniform and many unexpected neurons and axons are stimulated. The artificial stimulation should be spatiotemporally specified since it would dynamically change the neuronal network in an activity-dependent manner.

Optical stimulation methods have advantages over conventional electrical stimulation methods: fine spatiotemporal resolution and the relative harmlessness and convenience (Callaway and Yuste, 2002; Miesenböck, 2004). Recently, photostimulation using channelrhodopsin-2 (ChR2) has become a powerful tool for the investigation of neural networks both *in vivo* and *in vitro* (Boyden et al., 2005; Li et al., 2005; Ishizuka et al., 2006; Bi et al., 2006). A brief blue light illumination depolarizes the neurons, which are genetically engineered to express ChR2, over the threshold to evoke action potentials that are phase-locked with the light pulses. Neuronal activity can also be negatively regulated by light if the neurons are engineered to express either a Cl^--transporting rhodopsin, *e.g.* NpHR from *Natronomonas pharaonis* (Zhang et al., 2007; Han and Boyden, 2007) or an H^+-transporting rhodopsin, *e.g.* archaerhodopsin-3 from *Halorubrum sodomense* (Chow et al., 2010)

Abbreviations: ChR2, channelrhodopsin-2; ACSF, artificial cerebrospinal fluid; ArchT, archaerhodopsin from *Halorubrum* strain TP009; D-AP5, D-(−)-2-amino-5-phosphonovaleric acid; ΔIF_{50}, light-dependent shift of the current amplitude which Exhibits 50% fidelity; DMD, digital micro-mirror device; DNQX, 6,7-Dinitroquinoxaline-2,3-dione; GCL, granule cell layer; LED, light-emitting diode; NpHR, *Natronomonas pharaonis* halorhodopsin; PMOS, projector-managing optical system; ROI, region of interest; SL-M, stratum lacnosum-moleculare; SO, stratum oriens; SP, stratum pyramidale; SR, stratum radiatum.

* Corresponding author at: Department of Developmental Biology and Neurosciences, Tohoku University Graduate School of Life Sciences, Sendai 980-8577, Japan. Tel.: +81 22 217 6208; fax: +81 22 217 6211.
E-mail address: yawo-hiromu@m.tohoku.ac.jp (H. Yawo).

0168-0102/$ – see front matter © 2012 Elsevier Ireland Ltd and the Japan Neuroscience Society. All rights reserved.
doi:10.1016/j.neures.2012.03.009

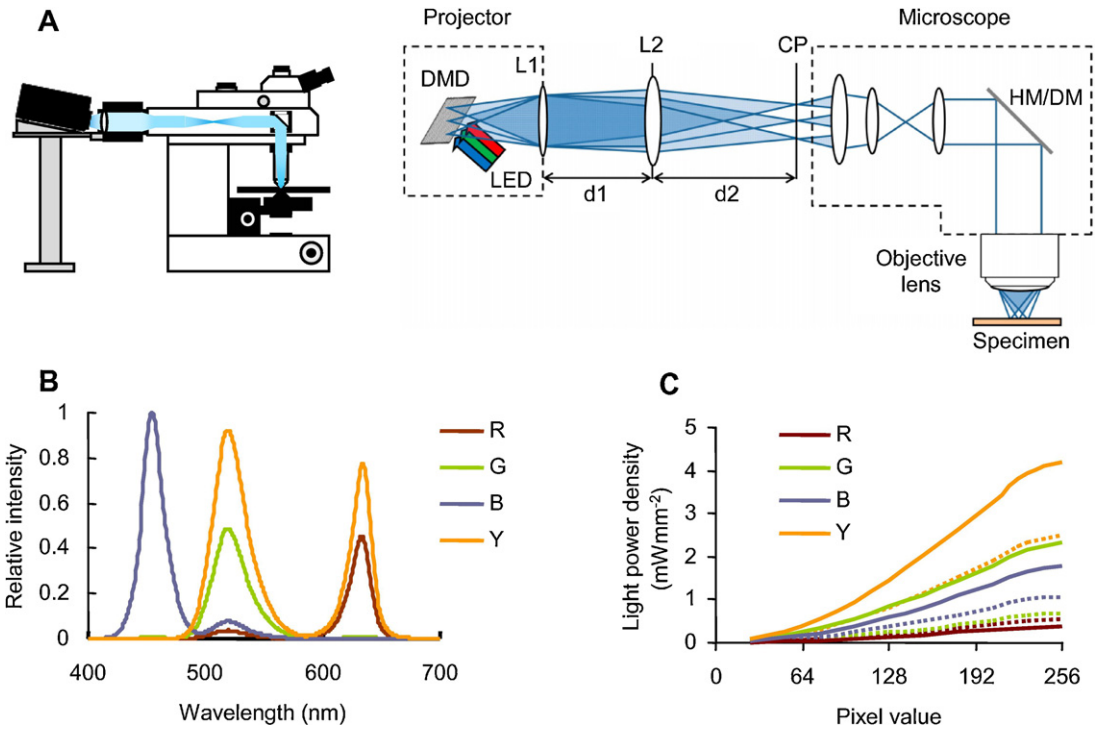

Fig. 1. Setup of the projector-managing optical system (PMOS). (A) The image made by a DMD-based projector is focused on the specimen through a focusing lens (L2), a half/dichroic mirror (HM/DM) and an objective lens. L1, projector lens. CP, conjugate plane. Here, d1 and d2 were, respectively, 70 and 90 mm. (B) Spectra of the projector's R-, G- and B-channel lights. That of the Y-channel light, which is a blend of the green and red lights, was also indicated. Relative value to the peak intensity of the B-channel light. (C) Light power density of R-, G-, B- and Y-channel irradiation was measured at the focal plane as a function of the pixel value using either the half mirror (dotted lines, 55% reflection) or the dichroic mirror (continuous lines, DM575), which reflects light with a wavelength <575 nm.

and archaerhodopsin-T (ArchT) from *Halorubrum* strain TP009 (Han et al., 2011). However, to achieve parallel photo-manipulations at multiple sites, an optimized optical system is necessary.

Previously, spatially patterned photostimulation methods using a laser scanning microscope have been employed for the functional mapping of the cortex (Wang et al., 2007a; Hira et al., 2009). Otherwise, the specimen was two-dimensionally targeted on a scanning stage under a single collimated laser beam (Ayling et al., 2009). In these studies, each targeted area was sequentially illuminated, but not simultaneously with other areas. Recently, two-dimensional array LEDs has been designed for patterned photostimulation (Grossman et al., 2010). At present, the irradiance would be uneven in a given field on the specimen because of the presence of inter-LED space. Nevertheless, this could become one of the most ideal tools given the high temporal resolution, high power and multiple colors. Spatial light modulators based on a digital micro-mirror device (DMD) have also been proposed as another ideal tool for patterned photostimulation, since they are currently employed for projecting multi-colored patterned images and each micro-mirror can be turned on and off at high frequencies up to several kHz. Actually, 380 and 505 nm LED lights were alternately applied on a region of interest (ROI) to switch on and off the light-sensitive ionotropic glutamate receptors (Wang et al., 2007b). The ChR2-expressing neurons were spatially differentiated from other neurons in the circuit using DMD array (Guo et al., 2009). Farah et al. (2007) applied a DMD-based commercial projector for the patterned activation of retinal ganglion cells that express ChR2. By using DMD, these studies could employ patterned photostimulation either temporally or spatially, but not both. Thus, until now, fine manipulation of spatiotemporally patterned parallel photostimulation has not yet been attained.

In this paper, we designed a microscope epi-illumination system that projects a spatially patterned image of a commercially available projector through an objective lens on the specimen. We also made a software program which enables one to adjust the projection to multiple targeted regions, to select the color of light and to switch it on and off in parallel with different temporal patterns. It is suggested that our projector-managing optical system (PMOS) would effectively facilitate the optogenetic analysis (Miller, 2006) of individual neurons and their circuits in brain slices and cultures.

A DMD-based commercial projector (K11, Acer Inc., Taipei, Taiwan) was mounted on the epi-illumination system of an upright microscope (FN-1, Nikon, Tokyo, Japan) (Fig. 1A). Its light source consists of red (630 ± 10 nm), green (520 ± 20 nm) and blue (455 ± 10 nm) light-emitting diodes (LEDs), which flickering alternately at 300 Hz. The projector image was conjugated by a focusing lens on the imaginary plane at the entrance of the epi-fluorescence tube and then focused on the specimen through a half/dichroic mirror and an objective lens (CFI75 LWD 16×W, Nikon). The projecting images were manipulated by our software (MiLSS 2.01) that was built on the Adobe Flash® (Adobe Systems, San Jose, CA). Circular ROIs of various diameters were multiply set in the field of view and assigned to one of three groups. Each group of ROIs turned on and off with a color-channel, irradiance and timing protocol independent of those of the other groups. Fig. 1B shows the spectra of the projected light measured by a spectrometer (C10083MD, Hamamatsu Photonics, Hamamatsu, Japan). The irradiance of each color channel, red (R), green (G), blue (B) or yellow (Y), was measured in the whole field of view at the microscope focus using a thermopile (MIR-100Q, Mitsubishi Chemical, Tokyo, Japan) as a function of the pixel value (Fig. 1C). However, the irradiance was uneven in the field of view in the range of 63–124% of the center brightness.

The performance of PMOS was evaluated using human embryonic kidney (HEK) 293 cells or acute rat hippocampal slices. HEK293 cells were grown under 5% CO_2 atmosphere at 37 °C in Dulbecco's modified Eagle's medium (Wako) supplemented

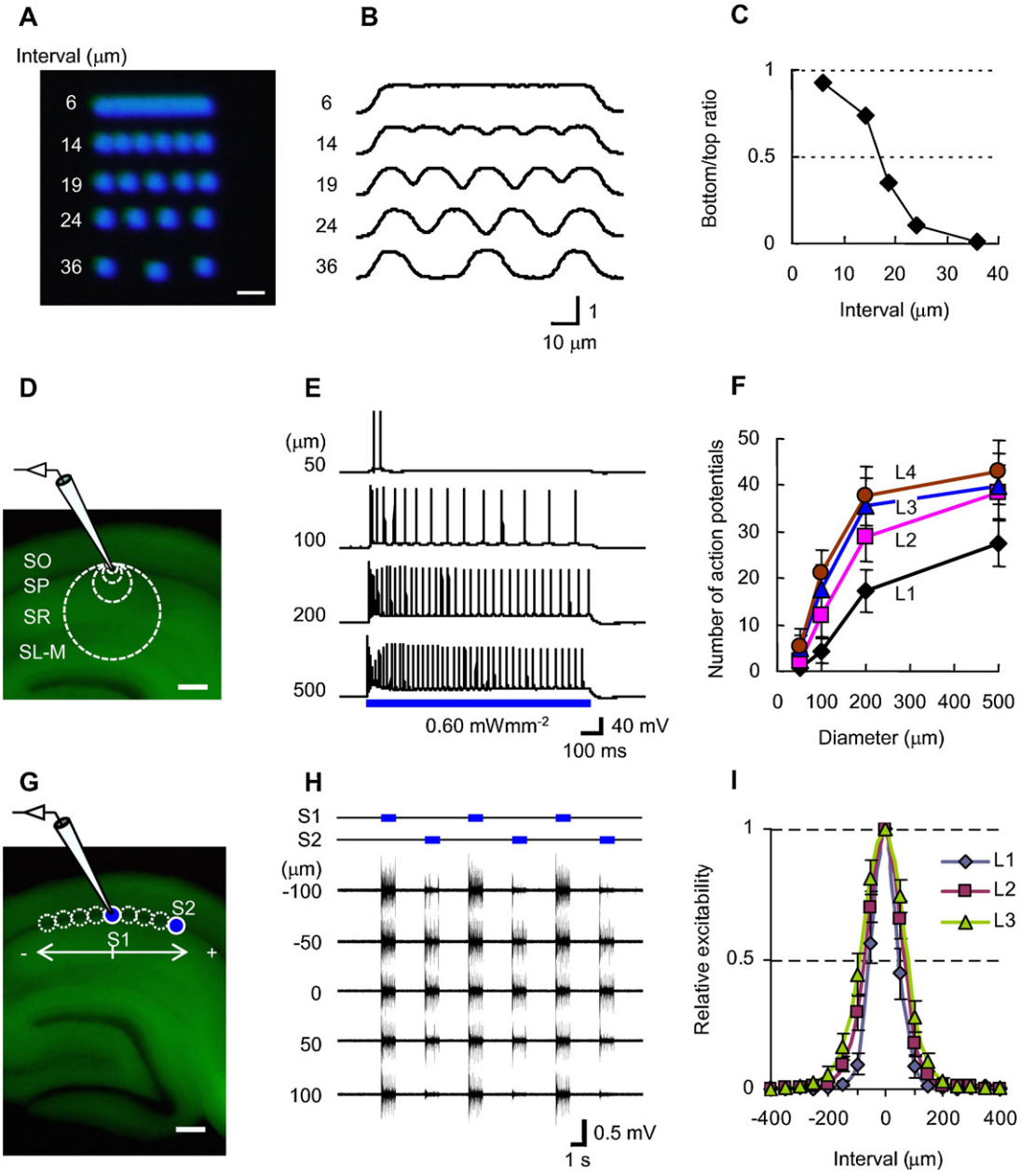

Fig. 2. Spatially patterned photostimulation. (A) Projection of light spots on the specimen. Each circular spot has a diameter of 13 μm. The numbers on the left indicate the center-to-center interval. (B) Center profiles of irradiance relative to the maximal values. (C) The bottom/top ratio of irradiance as a function of the center-to-center interval. (D) The size of blue-light ROI was changed while recording from a CA1 pyramidal cell in a hippocampal slice. The diameter of each circle is 50, 100, 200 or 500 μm. Note that this slice was made from the W-TChR2V4 transgenic rat in which CA1 pyramidal cells were expressing ChR2. (E) A series of typical records showing the effects of the ROI diameter with a given irradiance (0.60 mW mm^{-2}). (F) The number of action potentials of CA1 pyramidal cells evoked during a 1-s light pulse of a given irradiance (L1, 0.17 mW mm^{-2}; L2, 0.37 mW mm^{-2}; L3, 0.60 mW mm^{-2}; L4, 0.79 mW mm^{-2}) as a function of the ROI diameter (mean ± SEM, n = 5). (G) Test of spatial resolution using the slice. The recording electrode was placed in the center of S1 (diameter, 100 μm) where the blue light (duration, 1 s) was irradiated at 0.167 Hz. Another blue light ROI (S2; diameter, 100 μm, duration, 1 s) was moved along the pyramidal cell layer and shed alternately with S1. (H) Sample records of multi-unit spikes at CA1 while S1 and S2 were illuminated alternately. The numbers on the left are the center-to-center intervals between S1 and S2. (I) The number of spikes was counted during each light pulse and the average number evoked by S2 was expressed as relative to that of S1 and plotted against the center-to-center interval (mean ± SEM, n = 6). L1, 0.37 mW mm^{-2}; L2, 0.82 mW mm^{-2}; L3, 1.20 mW mm^{-2}. Scale bars, 20 μm in A and 200 μm in D and G. SO, stratum oriens; SP, stratum pyramidale; SR, stratum radiatum; SL-M, stratum lacunosum-moleculare.

with fetal bovine serum (10%). The cells were transfected with plasmids encoding ChR2 (Nagel et al., 2003) conjugated with *Venus* (Nagai et al., 2002) or ArchT conjugated with mCherry (Shaner et al., 2004) using Effectene transfection reagent (Qiagen, Tokyo, Japan). Electrophysiological recordings were conducted 72–96 h after transfection. Acute hippocampal slices (thickness, 300–400 μm) were made from 25 to 47 day-old thy1.2-ChR2-*Venus* transgenic rats (W-TChR2V4 line, Tomita et al., 2009) or the sindbis virus-transduced rats as described elsewhere (Wen et al., 2010). The recombinant sindbis pseudovirions, which include constructs of ArchT-mCherry, were made as described previously (Ishizuka et al., 2006). The viral solution (1.0×10^8 infectious particles/mL) was stereotaxically injected into the hippocampal dentate gyrus of 21 to 30-day-old Wistar rats: 3.8 mm posterior, 2.1 mm lateral and 2.9 mm ventral from the bregma. These rats were used in the experiments 12 h after transduction.

Electrophysiological recordings were made either through a whole-cell patch clamp or extracellularly using a conventional

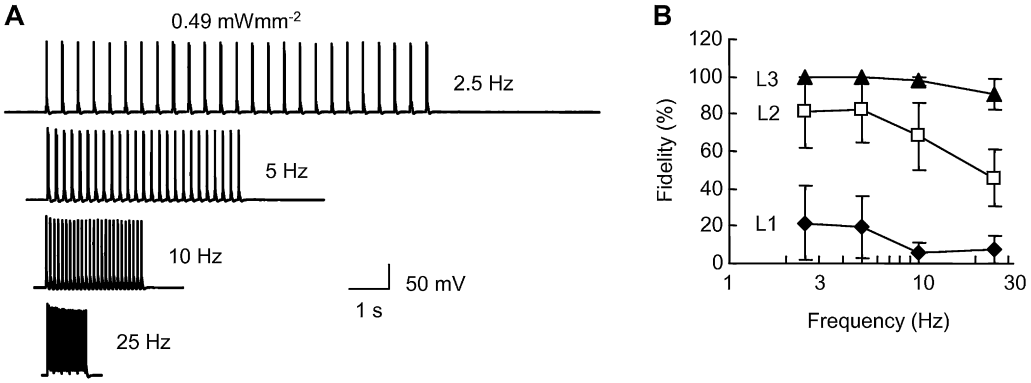

Fig. 3. Temporally patterned photostimulation. (A) Sample records from a CA1 pyramidal cell in the hippocampal slice made from the W-TChR2V4 transgenic rat. The blue light pulses (duration, 20 ms) were applied to the whole field of view at variable frequencies from 2.5 to 25 Hz. (B) The fidelity of generating action potential was plotted as a function of the frequency (mean ± SEM, $n = 5$). L1, 0.07 mW mm^{-2}; L2, 0.18 mW mm^{-2}; L3, 0.49 mW mm^{-2}.

system consisting of an amplifier, an A/D converter and software (Axopatch 200A, Digidata 1440A and Clampfit 10.3: Molecular Devices, Sunnyvale, CA). Multi-unit spikes were collected from the extracellular field potentials through a filter amplifier (FLA-01, Cygnus Technology, Southport, NC) and a digital high-pass filter at 300 Hz. The HEK293 cells were continuously perfused (1 ml/min) at room temperature (23–25 °C) with standard Tyrode solution containing (in mM), 138 NaCl, 3 KCl, 2 $CaCl_2$, 1 $MgCl_2$, 10 HEPES, 4 NaOH, 11 glucose (pH 7.4). The acute hippocampal slices were perfused at 34–35 °C with 2 ml/min normal artificial cerebrospinal fluid (ACSF) consisting of (in mM) 125 NaCl, 2.5 KCl, 26 $NaHCO_3$, 1.25 NaH_2PO_4, 2 $CaCl_2$, 1 $MgCl_2$, 11 glucose and pH 7.4 with 95% O_2 and 5% CO_2. The patch pipette solution contained (in mM) 120 CsOH, 100 glutamic acids, 50 HEPES, 5 EGTA, 2.5 $MgCl_2$, 2.5 MgATP, 0.1 leupeptin (PEPTIDE INSTITUTE, Osaka, Japan) (pH 7.3) for the voltage clamp or 125 K-gluconate, 10 KCl, 10 HEPES, 0.2 EGTA, 1 $MgCl_2$, 3 MgATP, 0.3 Na_2GTP, 10 Na_2 phosphocreatin, 0.1 leupeptin (pH 7.2) for the current clamp. For multi-unit recordings, glass pipettes filled with 1.78% Na_2SO_4 (0.7–0.8 MΩ) were placed in the CA1 pyramidal cell layer. In all slice experiments, ACSF contained 20 μM 6,7-Dinitroquinoxaline-2,3-dione (DNQX, Tocris Bioscience, Ellisville, MO), 25 μM D-(−)-2-amino-5-phosphonovaleric acid (D-AP5, Tocris), and 100 μM picrotoxin (Sigma–Aldrich, St. Louis, MO) to block synaptic inputs. The membrane potential was held at −40 mV during the voltage clamp experiments.

All animal experiments were performed according to the regulations for animal experiments and related activities at Tohoku University.

An array of circular spots of the minimal diameter (13 μm) were projected on the microscopic focal plain as shown in Fig. 2A and the relative irradiance was measured along the center line (Fig. 2B). The irradiance ratio of bottom/top was 50% with a center-to-center interval of 17 μm (Fig. 2C). However, the spatial resolution would be reduced by the scattering of light in thick tissue such as a brain slice. The effective resolution was tested using a slice of hippocampus from the W-TChR2V4 transgenic rat (Fig. 2D). The neural response was positively related to both the size of the ROI and the irradiance (Fig. 2E and F). Therefore, the populational activity of the CA1 pyramidal cell layer was recorded in response to a circular ROI (diameter, 100 μm) with a given irradiance while another ROI of the same size and irradiance was positioned at various distances along the CA1 pyramidal cell layer (Fig. 2G). As shown in Fig. 2H, the light-evoked firings were changed as a function of distance. The interval that exhibited 50% of the maximal response (Fig. 2I) was estimated to be 53 ± 4.7 μm with 0.37 mW mm^{-2}, 71 ± 6.0 μm with 0.82 mW mm^{-2} and 84 ± 6.8 μm with 1.20 mW mm^{-2} (mean ± SEM, $n = 6$).

When a blue light pulse of 20 ms duration was repetitively applied at the maximal frequency of our system (25 Hz), it robustly evoked depolarization of the neuronal membrane potential. However, the probability to evoke action potentials (fidelity) was dependent on both the frequency and irradiance. When the irradiance was relatively high, every depolarization was accompanied with the action potential in a typical CA1 pyramidal neuron of the W-TChR2V4 rat (Fig. 3A). However, the fidelity of action potential generation was reduced with the attenuation of irradiance at every frequency (Fig. 3B).

The power of the R-, G- and B-channel was adjusted to be equal and the photocurrents were measured from a ChR2-expressing HEK293 cell. As shown in Fig. 4A and B, the ChR2 photocurrent increased in the order of R < G < B. The effects of LED flickering were not manifest because of the relatively slow ChR2 kinetics (Ishizuka et al., 2006). Next, the following three ROIs of the same size (diameter, 200 μm) were set on the CA1 region of the slice and irradiated with the same pulse duration (100 ms) (Fig. 4C and D). The R-channel light was shed on the soma region and turned on every 1.2 s. The G-channel light was shed on the proximal region of the apical dendrite and turned on every 1.1 s. The B-channel light was shed on the distal region of the apical dendrite and turned on every 1 s. Each light pulse evoked small depolarization when the interval was relatively large. However, the depolarization was spatially summarized to evoke action potentials when the light pulses were temporally overlapped.

The enhanced green irradiation (520 ± 20 nm), which was irradiation of the Y-channel light through a dichroic mirror, DM575 (Fig. 1B and C), evoked a relatively large outward photocurrent in an ArchT-expressing HEK293 cell (Fig. 4E and F). The steady-state ArchT photocurrent density was 5.6 ± 1.1 pA pF^{-1} at the maximal irradiance (3.6 mW mm^{-2}), which was significantly larger than that evoked by the maximal B-channel light with DM575 (1.9 mW mm^{-2}). The notion that this green irradiation would reduce the excitability of an ArchT-expressing neuron through hyperpolarization was tested using dentate granule cells in the rat hippocampus (Fig. 4G), in which action potentials were evoked repetitively by injecting 10-ms depolarizing current pulses at 25 Hz. As shown in Fig. 4H, the enhanced green irradiation more effectively reduced the fidelity than the blue. The effects of LED flickering were not manifest because of the relatively large membrane time constant of the neuron. As the fidelity of generating action potentials was dependent on the amplitude of the injection current (Fig. 4I), we estimated the current amplitude that Exhibits 50% fidelity with 25 Hz and compared its light-dependent shift (ΔIF_{50}). The ΔIF_{50} by the above green irradiation was significantly larger than that by the blue (Fig. 4J). Therefore, our PMOS effectively

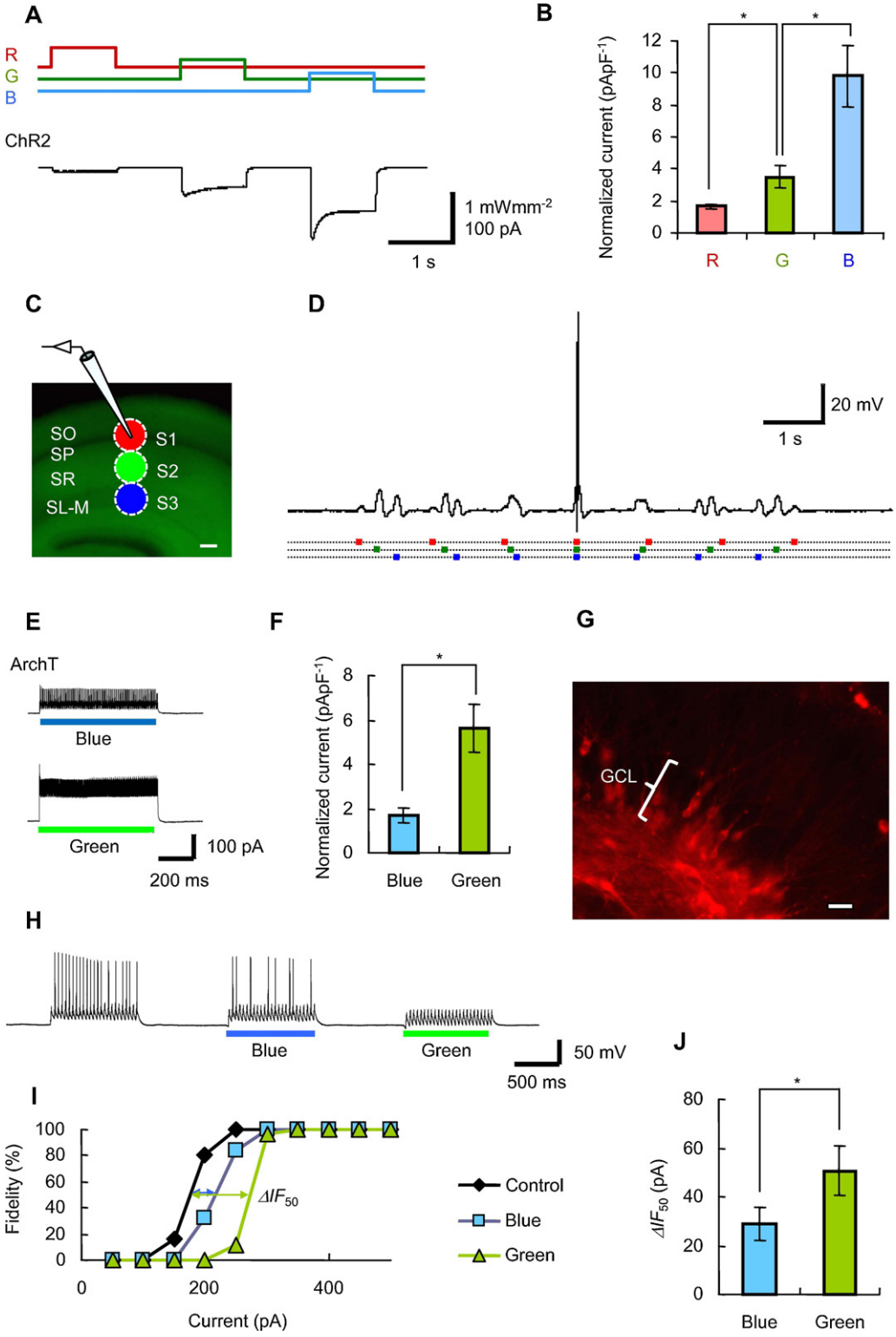

Fig. 4. Optical manipulation with discriminative wavelengths. (A) Sample record of ChR2 photocurrent while R-, G- or B-channel light pulses (duration, 1 s) was alternately irradiated on a HEK293 cell. (B) The peak ChR2 photocurrent evoked by the R-, G- or B-channel light was normalized by the cell's input capacitance and expressed as mean ± SEM ($n = 11$). *$P < 0.005$, Wilcoxon signed-ranks test. (C) While the light-evoked responses were recorded from a CA1 pyramidal cell of the W-TChR2V4 transgenic rat, three circular irradiating ROIs (S1–S3, diameter, each 200 μm) were set on the area covering the soma, the proximal and the distal part of the apical dendrite. (D) A typical response to the patterned irradiation of S1 (R-channel, 0.67 mW mm^{-2}), S2 (G-channel, 0.68 mW mm^{-2}) and S3 (B-channel, 0.67 mW mm^{-2}). (E) Sample record of photocurrent from an ArchT-expressing HEK293 cell while irradiated by blue (1.9 mW mm^{-2}) or green light (3.6 mW mm^{-2}). Since the ArchT photocurrent was fast in the ON/OFF kinetics, it fluctuated at 300 Hz as each LED was flickering. (F) The steady-state ArchT photocurrent evoked by blue (1.9 mW mm^{-2}) or green light (3.6 mW mm^{-2}) was normalized by the cell's input capacitance and expressed as mean ± SEM ($n = 10$). *$P < 0.005$, Wilcoxon signed-ranks test. (G) Light-evoked responses were recorded from dentate granule cells expressing ArchT-mCherry. (H) A typical response of a granule cell to the injected current pulses (20 pA) at 25 Hz. The suprathreshold responses (left) mostly became subthreshold with the simultaneous irradiation of the field of view with green light (right, 3.6 mW mm^{-2}), although it was less effective with blue light at maximal irradiance (middle, 1.9 mW mm^{-2}). (I) Fidelity of a GCL neuron in response to current injection (duration, 10 ms) at 25 Hz without (black diamond) or with blue (blue square) or green (green triangle) irradiation. (J) The current amplitude that exhibited 50% fidelity at 25 Hz was estimated and its light-dependent shift (ΔIF_{50}) was compared (mean ± SEM, $n = 9$). The positive shift by green light was significantly greater than that by blue light ($P < 0.005$, Wilcoxon signed-ranks test). Scale bars, 100 μm for C and 50 μm for G. GCL, granule cell layer.

manipulate the neuronal activity in a positive direction by the combination of ChR2 and blue irradiation and in a negative direction by the combination of ArchT and green irradiation.

The ability of our PMOS is limited by the present projector's properties such as spectrum and power of the source light, the LED flickering, the minimal ROI size (diameter, 13 μm) and the maximal frequency of the light pulse (25 Hz). However, using this projector, it was still possible to irradiate any place in the field of view with variable ROI sizes, to turn the light pulse on and off rapidly up to 25 Hz and to irradiate the groups of ROIs in parallel with different patterns, irradiance and wavelength. Our study suggests that the ChR2-expressing neurons in the brain slice are activated with enough high spatial resolution to differentiate individual neurons. Each neuron can be differentially irradiated with variable temporal patterns of either blue, green or red light although the light power density of blue or green irradiation was less than that for the maximal activation of ChR2 or ArchT with the present projector. The use of more powerful projectors would solve this problem since they could also be regulated by our software with minimal modifications. The spatiotemporal resolutions would be improved in the future by direct regulation of the DMD array with software using the present algorithm. In conclusion, our PMOS, combined with ChR2 or ArchT, would fulfill to some extent the requirements of artificial manipulation of neurons, namely generality, speed, localization and parallelism (Miesenböck, 2004).

The authors gratefully thank Drs. Georg Nagel, Edward S. Boyden, Atsushi Miyawaki and Roger Y. Tsien for the cDNA plasmids and B. Bell for language assistance. This work was supported by Grants-in-aid for scientific research from the Ministry of Education, Culture, Sports, Science and Technology (MEXT) of Japan, Global COE Program (Basic & Translational Research Center for Global Brain Science), MEXT, Strategic Research Program for Brain Sciences (SRPBS, MEXT) and by the Program for Promotion of Fundamental Studies in Health Sciences of the National Institute of Biomedical Innovation (NIBIO).

References

Ayling, O.G.S., Harrison, T.C., Boyd, J.D., Goroshkov, A., Murphy, T.H., 2009. Automated light-based mapping of motor cortex by photoactivation of channelrhodopsin-2 transgenic mice. J. Neurosci. Methods 6, 219–224.

Bi, A., Cui, J., Ma, Y.P., Olshevskaya, E., Pu, M., Dizhoor, A.M., Pan, Z.H., 2006. Ectopic expression of a microbial-type rhodopsin restores visual responses in mice with photoreceptor degeneration. Neuron 50, 23–33.

Boyden, E.S., Zhang, F., Bamberg, E., Nagel, G., Deisseroth, K., 2005. Millisecond-timescale, genetically targeted optical control of neural activity. Nat. Neurosci. 8, 1263–1268.

Callaway, E.M., Yuste, R., 2002. Stimulating neurons with light. Curr. Opin. Neurobiol. 12, 587–592.

Chow, B.Y., Han, X., Dobry, A.S., Qian, S., Chuong, A.S., Li, M., Henninger, M.A., Belfort, G.M., Lin, Y., Monahan, P.E., Boyden, E.S., 2010. High-performance genetically targetable optical neural silencing by light-driven proton pump. Nature 46, 98–102.

Farah, N., Reutsky, I., Shoham, S., 2007. Patterned optical activation of retinal ganglion cells. In: Conf. Proc. IEEE Eng. Med. Biol. Soc. 2007, pp. 6369–6371.

Grossman, N., Poher, V., Grubb, M.S., Kennedy, G.T., Nikolic, K., McGovern, B., Berlinguer Palmini, R., Gong, Z., Drakakis, E.M., Meil, M.A.A., Dawson, M.D., Burrone, J., Degenaar, P., 2010. Multi-site optical excitation using ChR2 and micro-LED array. J. Neural. Eng. 7, 016004.

Guo, Z.V., Hart, A.C., Ramanathan, S., 2009. Optical interrogation of neural circuits in *Caenorhabditis elegans*. Nat. Methods 6, 891–896.

Han, X., Boyden, E.S., 2007. Multiple-color optical activation, silencing, and desynchronization of neural activity, with single-spike temporal resolution. PLoS One 2, e299.

Han, X., Chow, B.Y., Zhou, H., Klapoetke, N.C., Chuong, A., Rajimehr, R., Yang, A., Baratta, M.V., Winkle, J., Desimone, R., Boyden, E.S., 2011. A high-light sensitivity optical neural silencer: development and application to optogenetic control of non-human primate cortex. Front. Syst. Neurosci. 5, 00018.

Hira, R., Honkura, N., Noguchi, J., Maruyama, Y., Augustine, G.J., Kasai, H., Matsuzaki, M., 2009. Transcranial optogenetic stimulation for functional mapping of the motor cortex. J. Neurosci. Methods 179, 258–263.

Ishizuka, T., Kakuda, M., Araki, R., Yawo, H., 2006. Kinetic evaluation of photosensitivity in genetically engineeredneurons expressing green algae light-gated channels. Neurosci. Res. 54, 85–94.

Li, X., Gutierrez, D.V., Hanson, M.G., Han, J., Mark, M.D., Chiel, H., Hegemann, P., Landmesser, L.T., Herlitze, S., 2005. Fast noninvasive activation and inhibition of neural and network activity by vertebrate rhodopsin and green algae channelrhodopsin. Proc. Natl. Acad. Sci. USA 102, 17816–17821.

Miesenböck, G., 2004. Genetic methods for illuminating the function of neural circuits. Curr. Opin. Neurobiol. 14, 395–402.

Miller, G., 2006. Shining new light on neural circuits. Science 314, 674–676.

Nagai, T., Ibata, K., Park, E.S., Kubota, M., Mikoshiba, K., Miyawaki, A., 2002. A variant of yellow fluorescent protein with fast and efficient maturation for cell-biological applications. Nat. Biotechnol. 20, 87–90.

Nagel, G., Szellas, T., Huhn, W., Kateriya, S., Adeishvili, N., Berthold, P., Ollig, D., Hegemann, P., Bamberg, E., 2003. Channelrhodopsin-2, a directly light-gated cation-selective membrane channel. Proc. Natl. Acad. Sci. USA 100, 13940–13945.

Shaner, N.C., Campbell, R.E., Steinbach, P.A., Giepmans, B.N.G., Palmer, A.E., Tsien, R.Y., 2004. Improved monomeric red, orange and yellow fluorescent proteins derived from Discosoma sp. red fluorescent protein. Nat. Biotechnol. 22, 1567–1572.

Tomita, H., Sugano, E., Fukazawa, Y., Isago, H., Sugiyama, Y., Hiroi, T., Ishizuka, T., Mushiake, H., Kato, M., Hirabayashi, M., Shigemoto, R., Yawo, H., Tamai, M., 2009. Visual properties of transgenic rats harboring the channelrhodopsin-2 gene regulated by the thy-1.2 promoter. PLoS One 4, e7679.

Wang, H., Peca, J., Matsuzaki, M., Matsuzaki, K., Noguchi, J., Qiu, L., Wang, D., Zhang, F., Boyden, E., Deisseroth, K., Kasai, H., Hall, W.C., Feng, G., Augustine, G.J., 2007a. High-speed mapping of synaptic connectivity using photostimulation in Channelrhodopsin-2 transgenic mice. Proc. Natl. Acad. Sci. USA 104, 8143–8148.

Wang, S., Szobota, S., Wang, Y., Volgraf, M., Liu, Z., Sun, C., Trauner, D., Isacoff, E.Y., Zhang, X., 2007b. All optical interface for parallel, remote, and spatiotemporal control of neuronal activity. Nano Lett. 7, 3859–3863.

Wen, L., Wang, H., Tanimoto, S., Egawa, R., Matsuzaka, Y., Mushiake, H., Ishizuka, T., Yawo, H., 2010. Opto-current-clamp actuation of cortical neurons using a strategically designed channelrhodopsin. PLoS One 5, e12893.

Zhang, F., Wang, L.P., Brauner, M., Liewald, J.F., Kay, K., Watzke, N., Wood, P.G., Bamberg, E., Nagel, G., Gottschalk, A., Deisseroth, K., 2007. Multimodal fast optical interrogation of neural circuitry. Nature 446, 633–639.